Effects of Vimentin Intermediate Filaments on the Structure and Dynamics of *In Vitro* Multicomponent Interpenetrating Cytoskeletal Networks

Yinan Shen,[1] Huayin Wu,[1] Peter J. Lu (陆述義),[1] Dianzhuo Wang,[1] Marjan Shayegan,[1] Hui Li,[2] Weichao Shi,[3] Zizhao Wang,[1] Li-Heng Cai,[4] Jing Xia,[1] Meng Zhang,[1,5] Ruihua Ding,[1,6] Harald Herrmann,[7,8] Robert Goldman,[9] Fred C. MacKintosh,[10] Arturo Moncho-Jordá,[11] and David A. Weitz[1,12]

[1]*Department of Physics & John A. Paulson School of Engineering and Applied Sciences, Harvard University, Cambridge, Massachusetts 02138, USA*
[2]*School of Systems Science, Beijing Normal University, Beijing 100875, China*
[3]*Key Laboratory of Functional Polymer Materials of the Ministry of Education, Institute of Polymer Chemistry, College of Chemistry, Nankai University, Tianjin 300071, China*
[4]*Materials Science and Engineering & Chemical Engineering, University of Virginia, Charlottesville, Virginia 22904, USA*
[5]*Precision Medicine Institute, The First Affiliated Hospital of Sun Yat-Sen University, Sun Yat-Sen University, Guangzhou 510080, China*
[6]*Department of Chemistry, University of Illinois at Urbana-Champaign, Urbana and Champaign, Illinois 61801, USA*
[7]*Division of Cell Biology, German Cancer Research Center (DKFZ), Heidelberg 69120, Germany*
[8]*Institute of Neuropathology, University Hospital Erlangen, Friedrich-Alexander Universität Erlangen-Nürnberg, Erlangen 91054, Germany*
[9]*Department of Cell and Developmental Biology, Northwestern University, Chicago, Illinois 60611, USA*
[10]*Department of Chemical and Biomolecular Engineering & Center for Theoretical Biological Physics, Rice University, Houston, Texas 77005, USA*
[11]*Department of Applied Physics & Institute Carlos I for Theoretical and Computational Physics, University of Granada, Granada 18071, Spain*
[12]*Wyss Institute for Biologically Inspired Engineering, Harvard University, Cambridge, Massachusetts 02138, USA*

(Received 20 December 2020; revised 1 June 2021; accepted 30 July 2021; published 3 September 2021)

We investigate the rheological properties of interpenetrating networks reconstituted from the main cytoskeletal components: filamentous actin, microtubules, and vimentin intermediate filaments. The elastic modulus is determined largely by actin, with little contribution from either microtubules or vimentin. However, vimentin dramatically impacts the relaxation, with even small amounts significantly increasing the relaxation time of the interpenetrating network. This highly unusual decoupling between dissipation and elasticity may reflect weak attractive interactions between vimentin and actin networks.

DOI: 10.1103/PhysRevLett.127.108101

The cytoskeleton of eukaryotic cells is composed of entangled filamentous proteins that provide structural support and mechanical stability, enabling cells to resist deformation [1–5]. It consists predominantly of three independent but interpenetrating networks (IPNs): filamentous actin (F-actin), microtubules, and intermediate filaments (IFs). Vimentin intermediate filaments (VIFs) are the most abundant IFs. Without F-actin or microtubules, cells die; consequently, these two cytoskeletal proteins have been studied extensively [6–10]. By contrast, IFs have not been as widely investigated. Knocking out IFs does not kill cells; however, mutations in IFs lead to many diseases [11,12]. Moreover, IFs are very important for cell mechanics; knocking them out substantially alters the mechanical behavior of cells [13–18]. The complexity of the cytoskeletal systems in live cells precludes direct probes of the specific role of IFs in mechanical behavior. For example, knocking out VIFs entirely from cells triggers a cascade of downstream intracellular chemical reactions whose effects are not fully known [19,20]. An alternative method to gain insight into the underlying contribution of each component to the mechanics is through studies of networks reconstituted from the proteins [21]. For example, studies of reconstituted actin networks demonstrate the contribution of single filament relaxation dynamics to the high-frequency linear elasticity of networks, whereas the force-extension relation of a single actin filament accounts for the nonlinear behavior of networks [22,23]. Similarly, a reconstituted network of pure microtubules exhibits elasticity that seems to reflect transient cross-link interactions between microtubules [24]. By contrast, *in vitro* VIF networks exhibit a distinctive behavior of high stretchability with hardening at large deformations to resist breakage [25,26]. In addition, studies of IPNs reconstituted from pairs of components probe the effects of one component on the mechanical properties of the other. For example, a study of networks composed of F-actin and VIFs displays either stiffening or weakening upon the

addition of VIFs, depending on the F-actin cross-linking density [27]. A reconstituted network containing both F-actin and microtubules enables direct measurement of F-actin fluctuations by probing the bending dynamics of microtubules embedded in an elastic medium [28]. However, a more complete understanding of the mechanical properties of cells demands a study of the behavior of the three major cytoskeletal components reconstituted together to form all three IPNs. Unfortunately, the chemical buffer conditions typically used to reconstitute each individual component are incompatible, precluding the formulation of mixed component IPNs. Consequently, the structure and mechanical behavior of such networks have never been explored, and the effects of interaction among the three components forming such an IPN are not known.

In this Letter, we report the formation of a reconstituted network containing physiologically relevant concentrations of all three cytoskeletal proteins: F-actin, microtubules, and VIFs. We characterize the structure of the IPN using scanning and transmission electron microscopy, as well as confocal fluorescence microscopy; we probe the network mechanical properties with two-point microrheology, using micrometer-sized particles embedded within the reconstituted networks. We find that the addition of VIFs to networks of F-actin and microtubules constrains the fluctuating motion of the probe particles, suggesting that VIF networks are more flexible and fill space more than the other two networks. The elastic modulus of the IPN is largely determined by the F-actin concentration; by contrast, neither microtubules nor VIFs affect the elastic modulus significantly. Instead, the addition of VIFs, even at very low concentrations, significantly increases the network relaxation time, transforming an otherwise liquidlike actin network into a solid. Such independent control of relaxation time, with no effect on the magnitude of the modulus, is rare and suggests a purely dissipative mechanism that does not impact elasticity and which may be induced by the weak molecular interactions between the VIF tail domain and F-actin. Our findings determine the contributions of each component of an IPN, providing important insights into their mechanical properties.

The assembly of IPNs requires polymerization of each of the proteins simultaneously; this is challenging because the buffers for each are not compatible with one another [25,27,29,30]. We find a combination of buffer components that allows each protein network to be individually reconstituted. For each sample, we prepare an assembly buffer at the required concentration. To this, we add the individual protein stock solutions at appropriate concentrations to produce the final solution. We equilibrate this mixture at 37 °C for 200 min to assemble the polymer networks.

We use transmission electron microscopy (TEM) to directly visualize the assembled networks [31]. The sample forms an IPN of all three components as shown in Fig. 1(a).

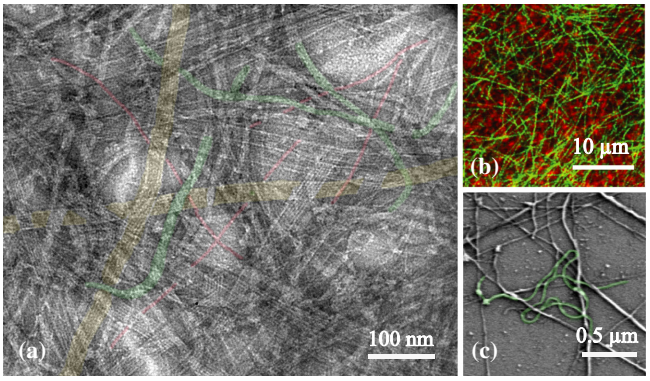

FIG. 1. (a) TEM image of a cytoskeletal network, containing F-actin (red), microtubules (yellow), and VIFs (green). (b) Confocal image of a network composed of 1 mg/mL F-actin (red), 1 mg/mL microtubules (green), and 0.5 mg/mL VIFs (unlabeled). (c) SEM image of the three-component cytoskeletal network. VIFs are colored green.

Each component has a distinct appearance: F-actin (red) has a helical structure and a diameter of 4–7 nm; microtubules (yellow) are thicker and striped; and VIFs (green) have a diameter between the other two.

To characterize the IPN in a more natural and dynamic state, we fluorescently label F-actin and microtubules. There is no fluorescence labeling method that maintains protein stability for VIFs. We use a confocal microscope (Leica TCS SP5) to image the reconstituted protein networks, and confirm that the polymers form IPNs, as shown in Fig. 1(b).

To investigate the network dynamics of the three cytoskeletal polymers, we add 1 μm-diameter fluorescent particles (F8823, Life Technologies) coated with polyethylene glycol to the mixture of the protein monomers at a final volume fraction of 10^{-3}. The sample chamber is maintained at 37 °C [31]. We image the particles using a wide field fluorescence microscope (Zeiss Axio Observer Z1) with a Complementary Metal Oxide Semiconductor (CMOS) camera (Hamamatsu Flash4.0 V3) and a 40X water-immersion objective, yielding 162.5 nm per pixel; for each sample run, we acquire 20 000 frames at 10 ms per frame. To minimize wall effects, we collect images 60 μm away from each coverslip. In each case, we prepare at least three samples and collect at least three videos at different places in each sample. To facilitate comparison, we set the concentration of each cytoskeletal component to be F-actin at 1 mg/mL (A), microtubules at 1 mg/mL (M), and VIFs at 0.5 mg/mL (V). We study samples of each of the three pairs, AM, AV and MV, as well as the sample of all three, AMV. For comparison, we also study samples of F-actin and VIFs alone, but not microtubules alone, since their network is not a solid.

To visualize the particle motion, we plot a heat map of the particle position distributions over time of all measured particle trajectories. We set the average position of each

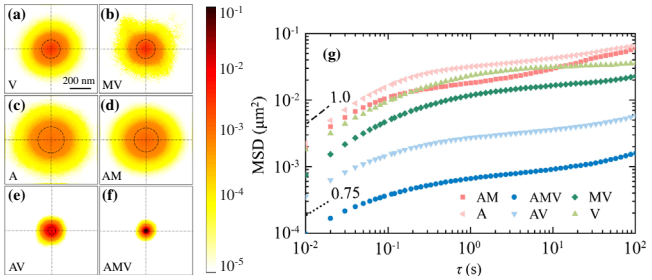

FIG. 2. (a)–(f) Two-dimensional heat maps of probability distributions of particle positions in various networks, showing the means (lines) and standard deviations $\bar{\sigma}$ (circles). Scale bar: 200 nm. Letters in legends represent network components. A: 1 mg/mL F-actin; M: 1 mg/mL microtubules; V: 0.5 mg/mL VIFs. (g) Time and ensemble-averaged mean-squared displacements of probe particles.

trajectory at the origin. The tracer particles are primarily constrained within the darker yellow area shown in Figs. 2(a)–2(f). We characterize the width of the distributions by the standard deviations, $\bar{\sigma}$. For V, $\bar{\sigma} = 122$ nm, as shown by the circle in Fig. 2(a). The addition of microtubules, MV, slightly increases confinement leading to $\bar{\sigma} = 118$ nm, as shown in Fig. 2(b). Compared with VIFs, the particles in the actin network, A, are less localized, $\bar{\sigma} = 169$ nm, as shown in Fig. 2(c). The addition of microtubules to the actin network, AM, has little effect on particle confinement, $\bar{\sigma} = 153$ nm, as shown in Fig. 2(d). However, when we combine VIFs and F-actin, AV, the particles are much more constrained, $\bar{\sigma} = 52$ nm, as shown in Fig. 2(e). The particles are even more constrained upon the addition of microtubules, AMV, $\bar{\sigma} = 24$ nm, as shown in Fig. 2(f). In each case, the microtubules only slightly increase confinement, as seen by comparing the left and right columns in Figs. 2(a)–2(f). By contrast, the combination of F-actin and VIFs leads to very strong confinement, as shown in Figs. 2(e) and 2(f).

To quantify the behavior, we calculate the particle mean-squared displacement (MSD). In all cases, the MSD rises at short τ and approaches a plateau, consistent with the heat maps, as shown in Fig. 2(g). The plateau values are consistent with the heat maps, with the two combinations containing VIFs, AV and AMV, having much lower plateau values of the MSD than do the others, and with AMV having an even lower value, as shown in Fig. 2(g). At very short τ, the MSD exhibits a power law dependence. For the samples with VIFs, the initial behavior is consistent with an exponent of 0.75, as shown in Fig. 2(g). By contrast, in the absence of VIFs, the data are more consistent with an initial viscous response and exponent of 1, as shown in Fig. 2(g). An exponent of 0.75 is expected for semiflexible networks at short times [36–39], although deviations from this are often observed for semiflexible networks when depletion effects lead to a decrease in concentration of the polymer in the immediate vicinity of the probe particles [40].

To more fully characterize the network, we determine its mechanical properties using microrheology. To mitigate the potential effects of depletion, we use two-point microrheology [35,41]. We cross-correlate displacements of pairs of tracer particles and determine the component along the line of the centers of paired particles. We apply the generalized Stokes-Einstein relation to obtain the viscoelastic properties of the cytoskeletal networks over four decades of frequency, f. For all samples, when the separation between the paired particles r is in the range of $3 < r < 25$ μm, the correlated motion along the line of the particles' centers is inversely proportional to r, indicating that the medium can be treated as homogeneous. All two-point microrheology measurements are performed within this region. At the intermediate frequency regime, the network is elastic, with the elastic modulus G' greater than the viscous modulus G''. The elastic modulus is weakly frequency dependent, $G' \sim f^{0.1}$, and we define the plateau elastic modulus G_0 at the center of the range. At high frequencies, $G'' > G'$ and $G'' \sim f^{0.75}$ for all data as shown in Figs. 3(a)–3(d). At low frequencies, G'' increases to a peak and then decreases with decreasing f, but remains greater than G'; this behavior reflects the low-frequency relaxation of the network. We define the relaxation time τ_r as the inverse of the frequency where $G' = G''$. These characteristics are typical of semiflexible polymers, and the functional form of the rheological behavior can be quantitatively captured by theories for semiflexible polymer networks [42]. The sample with pure VIFs is a very weak but still elastic network with $G_0 \sim 0.03$ Pa, as shown by the gray symbols in Fig. 3(d), consistent with the large plateau in the MSD and the broad heat map in Fig. 2. By contrast, the sample with a combination of F-actin and microtubules has a much larger $G_0 \sim 0.7$ Pa. This is in sharp contrast with the behavior expected from the constraints in the data in Fig. 2, where the AM sample is very close to the V sample. This confirms the presence of depletion effects and validates our use of two-point microrheology. Similar behavior is observed for the sample with only F-actin.

To explore the consequences of VIFs on rheological properties, we fix the F-actin concentration c_A at 1 mg/mL and the microtubule concentration c_M at 1 mg/mL, and vary the VIF concentration c_V in three-component networks. As c_V rises, G_0 increases only slightly, as shown by the blue lines in Figs. 3(a)–3(d). The change of G_0 is less than 0.5 Pa as c_V is varied from 0 to 0.7 mg/mL, as shown in Fig. 4(a). By contrast, the crossover frequency is lowered significantly as we add VIFs, reflecting a considerable increase in the network relaxation time, as shown by the red lines in Figs. 3(a)–3(d). We find that τ_r increases about tenfold over the range of c_V measured, as shown in Fig. 4(b). To qualitatively understand this behavior, we consider the relaxation of an individual actin filament, which is due to reptation in a "tube" formed by neighboring filaments [43,44], as shown schematically in the insert of

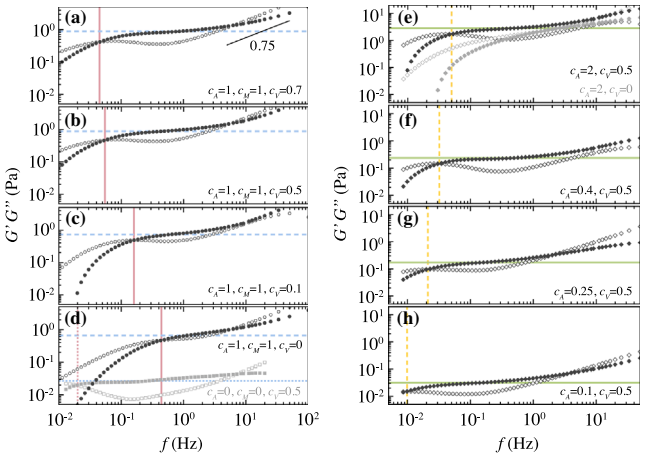

FIG. 3. (a)-(d) Frequency-dependent elastic moduli $G'(f)$ (solid symbols) and loss moduli $G''(f)$ (open symbols) of three-component cytoskeletal networks. Concentrations labeled in mg/mL in lower right, A: F-actin; M: microtubules; V: VIFs. Blue lines in (a)–(d) indicate plateau elastic moduli, which barely change with c_V. Network crossover frequency (red lines) decreases as c_V increases. (e)–(h) Frequency-dependent rheological properties of VIF-F-actin networks. Relaxation time (yellow lines) decreases as c_A increases, while plateau elastic modulus (green lines) increases with c_A. Concentrations are labeled in mg/mL in lower right.

Fig. 4(d). The addition of VIF adds additional constraints for the relaxation of the F-actin. This is consistent with the scanning electron microscopy (SEM) imaging of the three-component cytoskeletal networks, which shows VIFs wrapping around and contacting the other cytoskeletal filaments, as shown in Fig. 1(c). Surprisingly, however, the additional constraints due to the VIFs within the reptation tube do not significantly alter G_0; this is because the VIF network is so soft. Instead, the VIF network only slows the relaxation of F-actin. This behavior is highly unusual as typically relaxation and elasticity are coupled. This must reflect some form of viscous dissipation, which could arise from the weak interactions between the VIF tail domain and F-actin [45].

To explore the nature of the elastic behavior, we investigate the role of F-actin and the addition of VIFs. We consider only an IPN of F-actin and VIFs, because microtubules have a smaller effect in the IPN. This is clearly seen, for example, in the data for the mixed network with $c_A = 1$ mg/mL, $c_M = 1$ mg/mL, and $c_V = 0.5$ mg/mL, shown in Fig. 3(b). The elastic moduli remain nearly identical when microtubules are removed, with only a slight change in the low-frequency relaxation [31]. This behavior is also consistent with the observation that microtubules do not affect the linear elasticity of IPNs of F-actin and microtubules [46].

For reference, we measure the frequency-dependent rheological properties of a pure F-actin network at 2 mg/mL. The plateau in the intermediate frequency regime is barely discernible, indicating that the network is almost liquidlike, as shown by the solid gray circles in Fig. 3(e). However, upon addition of only a small amount of VIFs, $c_V = 0.5$ mg/mL, the F-actin network becomes dramatically more solidlike; the relaxation time becomes much longer, and the storage modulus remains independent of frequency over a much longer range; nevertheless, there is only a slight increase in G_0, as shown in Fig. 3(e). The addition of VIFs to form an IPN has a dramatic effect extending well beyond a direct addition of the two moduli [34]; although the VIF moduli are much less than those of F-actin, their sum has a dramatically different shape [31]. The effects of VIFs on the IPNs become even more pronounced as c_A is decreased: The F-actin networks become even more liquidlike and cannot be measured by our microrheology method, because the probe particles sediment too rapidly. Nevertheless, with the addition of VIFs at $c_V = 0.5$ mg/mL, the IPN remains solidlike over an extended frequency range, again reflecting the synergistic interaction of the two components, rather than a direct sum of the moduli.

As c_A decreases, G_0 of the IPN decreases significantly and is dominated by the contribution of F-actin, as shown by the solid green lines in Figs. 3(e)–3(h). The behavior of G_0 follows a power law in c_A with an exponent of about 1.5, as shown in Fig. 4(c); this value is smaller than that of pure actin networks, which is ~2.2 [22,25]. Although the networks remain solid, the relaxation becomes faster as c_A increases, as shown by the yellow lines in Figs. 3(e)–3(h). As c_A increases, τ_r initially decreases sharply, but then goes through a minimum and begins to increase again, as shown in Fig. 4(d). We attribute the initial sharp decrease to the increase in c_A, which dilutes the relative number of VIF-F-actin contacts imposed by the fixed concentration of VIFs. The increase in τ_r at the highest c_A reflects the contribution of the F-actin itself, which increases the network elastic modulus.

The addition of a VIF network that interpenetrates an actin network results in a dramatic increase in the solidlike character of the actin network, not through an increase in the elastic modulus, but through a significant increase in the relaxation time. This behavior could have very significant consequences for the networks in cells. To explore this possibility, we add myosin motors to the actin networks in the presence of the VIF and determine the contractility of the actomyosin complex. Initially, the activity of the myosin is inhibited by the addition of blebbistatin. We use a 488-nm laser to abolish this inhibition and allow the contractility to commence. The presence of VIF networks leads to much more rapid actomyosin contractility and results in a significantly more dense contracted structure, as shown in the three videos in Supplemental Material [31]. This is consistent with the behavior expected for a more solidlike network, confirming that the VIF also has an essential effect on a contractile actomyosin network. In

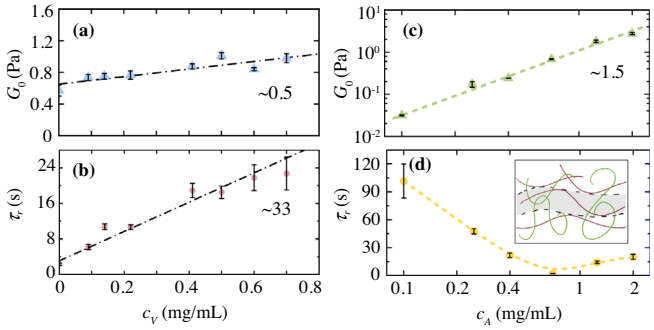

FIG. 4. (a) Plateau elastic modulus G_0 and (b) relaxation time τ_r variation with VIF concentration c_V for the network containing 1 mg/mL F-actin and 1 mg/mL microtubules. (c) G_0 and (d) τ_r variation with c_A in VIF-F-actin networks, with c_V fixed at 0.5 mg/mL. Yellow line in (d) is a B-spline fit. The insert in (d) depicts the reptation tube (gray) of an actin filament. Red: F-actin. Green: VIFs.

addition, since F-actin in cells is always cross-linked, we investigate an IPN consisting of 1 mg/mL microtubules and 1 mg/mL F-actin cross-linked with 1% biotinylated actin and streptavidin; upon the addition of 0.5 mg/mL VIF, the three-component IPN becomes more solidlike, but G_0 does not change appreciably.

The results presented in this Letter highlight the essential contribution of VIFs to the rheological properties of IPNs. The VIFs do not significantly contribute to the plateau elastic modulus of the network; instead, they extend the elastic regime to longer timescales, leading to a significant increase in the network relaxation time. Such an increase in the relaxation time, with no concomitant increase in the plateau elastic modulus is very unusual, as these two quantities are normally coupled and change simultaneously. The structural interactions between VIFs and F-actin in cells can modify the relaxation time by contributing to local molecular crowding in cytoskeletal networks. The interplay between the two networks also facilitates contraction induced by motor proteins. These results help rationalize the complex behavior of VIFs in cells, where they are reported to impact cell motility [14,15]. Given that the primary contribution of VIFs to cell mechanics is at long timescales, VIFs may play a key mechanical role in cells that undergo cancer metastasis, wound healing, or other slow dynamical physiological processes.

We gratefully acknowledge Thomas C. Ferrante and Xinyu Li for help with collection and analysis of microrheology data, and Adrian Pegoraro and Sijie Sun for valuable discussions. This work was supported by the NIH (2P01GM096971, 5P01HL120839), the Harvard MRSEC (DMR-1420570), the Harvard NSF-Simons Center for Mathematical and Statistical Analysis of Biology supported by NSF (DMS-1764269), and the Harvard FAS Quantitative Biology Initiative. F. C. M. acknowledges NSF DMR-1826623 and NSF PHY-2019745. A. M.-J. thanks the Fulbright Program in Spain and the "Plan Andaluz de Investigación, Desarrollo e Innovación" of the Junta de Andalucía (Project PY20_00241) for financial support. M. S. thanks the Fonds de recherche du Québec—Nature et technologies (FRQNT) for funding.

[1] N. Wang, J. P. Butler, and D. E. Ingber, Science **260**, 1124 (1993).
[2] K. E. Kasza, A. C. Rowat, J. Liu, T. E. Angelini, C. P. Brangwynne, G. H. Koenderink, and D. A. Weitz, Curr. Opin. Cell Biol. **19**, 101 (2007).
[3] D. A. Fletcher and R. D. Mullins, Nature (London) **463**, 485 (2010).
[4] T. Hohmann and F. Dehghani, Cells **8**, 362 (2019).
[5] J. S. Park, C. J. Burckhardt, R. Lazcano, L. M. Solis, T. Isogai, L. Li, C. S. Chen, B. Gao, J. D. Minna, R. Bachoo, R. J. DeBerardinis, and G. Danuser, Nature (London) **578**, 621 (2020).
[6] L. Blanchoin, R. Boujemaa-Paterski, C. Sykes, and J. Plastino, Physiol. Rev. **94**, 235 (2014).
[7] G. Salbreux, G. Charras, and E. Paluch, Trends Cell Biol. **22**, 536 (2012).
[8] S. Etienne-Manneville, Annu. Rev. Cell Dev. Biol. **29**, 471 (2013).
[9] J. H. Shin, M. L. Gardel, L. Mahadevan, P. Matsudaira, and D. A. Weitz, Proc. Natl. Acad. Sci. U.S.A. **101**, 9636 (2004).
[10] M. Dogterom and G. H. Koenderink, Nat. Rev. Mol. Cell Biol. **20**, 38 (2019).
[11] F. Danielsson, M. K. Peterson, H. Caldeira Araújo, F. Lautenschläger, and A. K. B. Gad, Cells **7**, 147 (2018).
[12] H. Herrmann, H. Bär, L. Kreplak, S. V. Strelkov, and U. Aebi, Nat. Rev. Mol. Cell Biol. **8**, 562 (2007).
[13] A. E. Patteson, A. Vahabikashi, K. Pogoda, S. A. Adam, K. Mandal, M. Kittisopikul, S. Sivagurunathan, A. Goldman, R. D. Goldman, and P. A. Janmey, J. Cell Biol. **218**, 4079 (2019).
[14] M. G. Mendez, S.-I. Kojima, and R. D. Goldman, FASEB J. **24**, 1838 (2010).
[15] B. Eckes, D. Dogic, E. Colucci-Guyon, N. Wang, A. Maniotis, D. Ingber, A. Merckling, F. Langa, M. Aumailley, and A. Delouvée, J. Cell Sci. **111**, 1897 (1998).
[16] N. Wang and D. Stamenovic, Am. J. Physiol.-Cell Physiol. **279**, C188 (2000).
[17] J. Lowery, E. R. Kuczmarski, H. Herrmann, and R. D. Goldman, J. Biol. Chem. **290**, 17145 (2015).
[18] M. Guo, A. J. Ehrlicher, S. Mahammad, H. Fabich, M. H. Jensen, J. R. Moore, J. J. Fredberg, R. D. Goldman, and D. A. Weitz, Biophys. J. **105**, 1562 (2013).
[19] Y. Jiu, J. Peränen, N. Schaible, F. Cheng, J. E. Eriksson, R. Krishnan, and P. Lappalainen, J. Cell Sci. **130**, 892 (2017).
[20] B. Langlois, E. Belozertseva, A. Parlakian, M. Bourhim, J. Gao-Li, J. Blanc, L. Tian, D. Coletti, C. Labat, Z. Ramdame-Cherif, P. Challande, V. Regnault, P. Lacolley, and Z. Li, Sci. Rep. **7**, 11628 (2017).
[21] A. R. Bausch and K. Kroy, Nat. Phys. **2**, 231 (2006).
[22] M. L. Gardel, J. H. Shin, F. C. MacKintosh, L. Mahadevan, P. Matsudaira, and D. A. Weitz, Science **304**, 1301 (2004).

[23] M. L. Gardel, J. H. Shin, F. C. MacKintosh, L. Mahadevan, P. A. Matsudaira, and D. A. Weitz, Phys. Rev. Lett. **93**, 188102 (2004).
[24] Y.-C. Lin, G. H. Koenderink, F. C. MacKintosh, and D. A. Weitz, Macromolecules **40**, 7714 (2007).
[25] P. A. Janmey, U. Euteneuer, P. Traub, and M. Schliwa, J. Cell Biol. **113**, 155 (1991).
[26] J. Hu, Y. Li, Y. Hao, T. Zheng, S. K. Gupta, G. A. Parada, H. Wu, S. Lin, S. Wang, X. Zhao, R. D. Goldman, S. Cai, and M. Guo, Proc. Natl. Acad. Sci. U.S.A. **116**, 17175 (2019).
[27] M. H. Jensen, E. J. Morris, R. D. Goldman, and D. A. Weitz, BioArchitecture **4**, 138 (2014).
[28] C. P. Brangwynne, G. H. Koenderink, F. C. MacKintosh, and D. A. Weitz, Phys. Rev. Lett. **100**, 118104 (2008).
[29] M. Inagaki, Y. Gonda, M. Matsuyama, K. Nishizawa, Y. Nishi, and C. Sato, J. Biol. Chem. **263**, 5970 (1988).
[30] M. P. López, F. Huber, I. Grigoriev, M. O. Steinmetz, A. Akhmanova, M. Dogterom, and G. H. Koenderink, Methods Enzymol. **540**, 301 (2014).
[31] See Supplemental Material at http://link.aps.org/supplemental/10.1103/PhysRevLett.127.108101 for supporting information, which includes Refs. [32–35].
[32] H. Herrmann, I. Hofmann, and W. W. Franke, J. Mol. Biol. **223**, 637 (1992).
[33] H. Wu, Y. Shen, D. Wang, H. Herrmann, R. D. Goldman, and D. A. Weitz, Biophys. J. **119**, 55 (2020).
[34] T. Golde, C. Huster, M. Glaser, T. Händler, H. Herrmann, J. A. Käs, and J. Schnauß, Soft Matter **14**, 7970 (2018).
[35] J. C. Crocker, M. T. Valentine, E. R. Weeks, T. Gisler, P. D. Kaplan, A. G. Yodh, and D. A. Weitz, Phys. Rev. Lett. **85**, 888 (2000).
[36] F. Gittes, B. Schnurr, P. D. Olmsted, F. C. MacKintosh, and C. F. Schmidt, Phys. Rev. Lett. **79**, 3286 (1997).
[37] B. Schnurr, F. Gittes, F. C. Mackintosh, and C. F. Schmidt, Macromolecules **30**, 7781 (1997).
[38] D. C. Morse, Phys. Rev. E **58**, R1237 (1998).
[39] F. Gittes and F. C. MacKintosh, Phys. Rev. E **58**, R1241 (1998).
[40] B. S. Chae and E. M. Furst, Langmuir **21**, 3084 (2005).
[41] M. T. Valentine, P. D. Kaplan, D. Thota, J. C. Crocker, T. Gisler, R. K. Prud'homme, M. Beck, and D. A. Weitz, Phys. Rev. E **64**, 061506 (2001).
[42] C. P. Broedersz and F. C. MacKintosh, Rev. Mod. Phys. **86**, 995 (2014).
[43] P. G. De Gennes, J. Chem. Phys. **55**, 572 (1971).
[44] J. A. Kas, H. H. Strey, and E. Sackmann, Nature (London) **368**, 226 (1994).
[45] R. B. Cary, M. W. Klymkowsky, R. M. Evans, A. Domingo, J. A. Dent, and L. E. Backhus, J. Cell Sci. **107**, 1609 (1994).
[46] Y.-C. Lin, G. H. Koenderink, F. C. MacKintosh, and D. A. Weitz, Soft Matter **7**, 902 (2011).